

PACS numbers: 42.55.Px; 42.60.Lh
DOI: 10.1070/QE2008v038n09ABEH013814

Emission of zinc selenide plates excited by a pulsed electric field

K.V. Berezhnoi, A.S. Nasibov, P.V. Shapkin, V.G. Shpak, S.A. Shunailov, M.I. Yalandin

***Abstract*. The emission power of zinc selenide plates placed in the air gap between electrodes is determined as a function of the amplitude of applied high-voltage nanosecond pulses and the gap width. The laser emission spectra of samples excited by an electron beam and an electric field are presented. The influence of the electrode shape on the emission pattern is studied. An increase in a laser pulse duration compared to the duration of an exciting high-voltage pulse was observed. It is assumed that this is explained by recombination emission processes proceeding in a dense electron – hole plasma.**

Keywords: *streamer lasers, electron-beam-pumped lasers, zinc selenide, electroluminescence, subnanosecond high-voltage pulses.*

1. Introduction

The irradiation of plane – parallel zinc selenide single-crystal plates grown by oversublimation from a gas phase by picosecond high-voltage pulses was studied for the first time in [1]. The use of pulse durations of hundreds of picoseconds with the amplitude of up to 240 kV made in possible to increase considerably the breakdown voltage and to decrease the gap between the cathode and anode, where zinc selenide plates were placed, thereby increasing considerably the electric field strength in the cathode – anode gap. Another advantage of using ultrashort pulses is the possibility of investigating samples in gases without placing them into a liquid dielectric. A discharge in gas provides the additional irradiation of samples by UV light and an electron beam produced during a rapid increase in the amplitude of a high-voltage pulse [2]. The first experiments on the stimulated emission of zinc selenide under the above-mentioned conditions showed [1] that, unlike streamer lasers [3 – 6], a discharge was predominantly observed along the electric field direction, the lasing region increased, and the radiation directivity improved.

K.V. Berezhnoi, A.S. Nasibov, P.V. Shapkin P.N. Lebedev Physics Institute, Russian Academy of Sciences, Leninsky prosp. 53, 119991 Moscow, Russia; e-mail: nasibov@sci.lebedev.ru;
V.G. Shpak, S.A. Shunailov, M.I. Yalandin Institute of Electrophysics, Ural Branch, Russian Academy of Sciences, ul. Amundsena 106, 620016 Ekaterinburg, Russia

Received 5 February 2008; revision received 22 May 2008
Kvantovaya Elektronika **38** (9) 829 – 832 (2008)
Translated by M.N. Sapozhnikov

In this paper, we determined the dependence of the emission power of zinc selenide plates of different thicknesses on the incident pulse amplitude and the gap width between a sample and the anode. The lasing spectra of the plates excited by an electron beam and an electric field are presented and the influence of the electrode shape on the emission spectrum is demonstrated.

2. Experimental

The basic component of our experimental setup was a RADAN-303B nanosecond pulse generator [7] with a picosecond energy compression unit [8] and a coaxial attachment manufactured for these experiments. The picosecond unit provided the control of the pulse amplitude U_0 from 20 to 250 kV in a wave propagating in a transmission line with a wave resistance of 45 Ω in the direction of the coaxial attachment. The transmission line was connected with the attachment along the axis on which the cathode and anode were placed in series. The coaxial attachment was a coaxial of diameter 7 cm and length ~4 cm, with an electrode of diameter 2 cm placed on its axis, which was ended by the cathode. The coaxial attachment design provided the rapid changing of the cathode and anode and of the gap between them. The anode had holes and the coaxial attachment had side slits for measuring the emission parameters and emission photographing. Most of the experiments were performed for $U_0 \leqslant 130$ kV and pulse durations of 400 – 500 ps. The pulse shape and their amplitude U_0 were measured with a capacitive divider with distributed parameters, which was built in the transmission line.

The scheme of excitation of single-crystal ZnSe plates by subnanosecond pulses is shown in Fig. 1. Plane – parallel

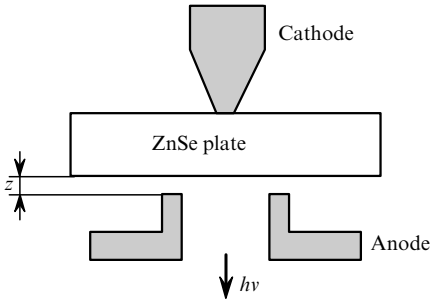

Figure 1. Scheme of excitation of ZnSe plates by high-voltage nanosecond pulses.

ZnSe plates of different thicknesses and shapes were placed opposite the cathode tightly pressed to them. The movable circular anode was placed at a distance of $z = 0 - 10$ mm from the plate plane. The emission was observed and optical parameters were measured through an axial hole in the anode. The pulsed emission power was measured with a FEK-22 coaxial photocell and a broadband FP-70S photodiode with a fibre input. The emission spectrum was recorded with an FSD-8 minispectrometer with a resolution of 1 nm. Voltage and light pulses were recorded with a broadband 6-GHz Tektronix TDS 6604 oscilloscope. The results obtained by exciting lasing by the electric field and electron beam were compared by replacing the coaxial attachment by a chamber from which the laser beam was coupled out to air through a foil [2].

3. Experimental results

Emission power. The typical shape of a voltage pulse propagated in the transmission line toward the cathode and the light pulse shape are shown in Fig. 2. The duration and shape of light and voltage pulses were different. The increase in the light pulse duration compared to that of the high-voltage pulse was also observed upon excitation of crystals by a high-power electron beam (Fig. 3). The characteristic pulse elongation time was ~ 3.5 ns. The possible reasons for the light pulse elongation will be considered below.

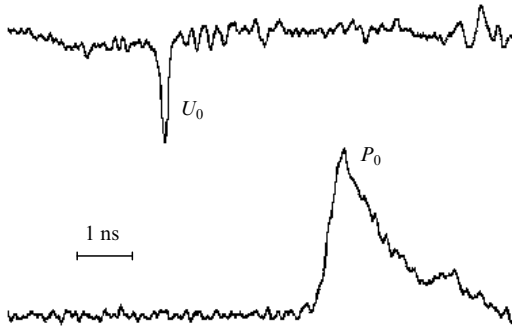

Figure 2. Voltage pulse with the amplitude $U_0 = 54$ kV and the light pulse of power $P_0 = 210$ W observed upon pumping a 0.3-mm-thick ZnSe plate by the electric field.

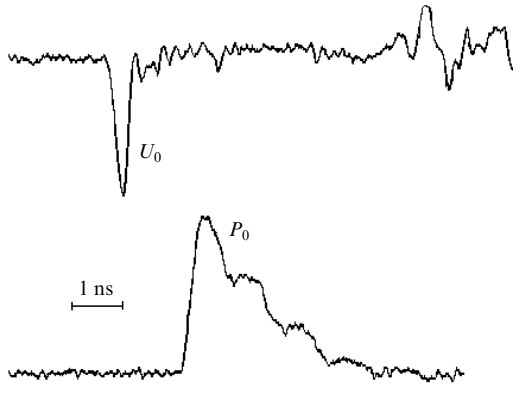

Figure 3. Accelerating voltage pulse ($U_0 = 148$ kV, the current density is 500 A cm^{-2}) and the 555-nm laser pulse of power P_0 observed upon pumping a 50-μm-thick CdSSe single-crystal plate by an electron beam.

Figure 4 shows the dependences of the peak emission power of ZnSe plates of thickness 0.3, 0.7, and 1.2 mm on U_0 for the gap between a plate and the anode $z = 2$ mm. The first two samples were polished chemically and mechanically, while the third one – only mechanically. Thin plates were excited by using the cathode in the form of a truncated cone with the apex of diameter 1 mm, while the 1.2-mm-thick plate was studied by using the cylindrical cathode and anode with the ratio of diameters 2 mm : 1mm and 5 mm : 3 mm, respectively. Figure 5 presents the dependences of the emission power of ZnSe plates of different thicknesses on the gap z for different U_0. One can see from Figs 4 and 5 that the slope of the growth in the emission power increases with decreasing the plate thickness, while the lasing threshold lies within $10 - 15$ kV. The maximum light pulse energy did not exceed 5×10^{-7} J.

Spectral parameters. After the achievement of the lasing threshold, the half-width of the spectrum decreased down to 3 nm and then increased up to 10 nm with increasing U_0 from 20 to 150 kV. This was accompanied by the red shift of the emission band to $480 - 482$ nm. Such an increase in the lasing bandwidth and the red shift of the emission band are typical for streamer and electron-beam-pumped lasers and

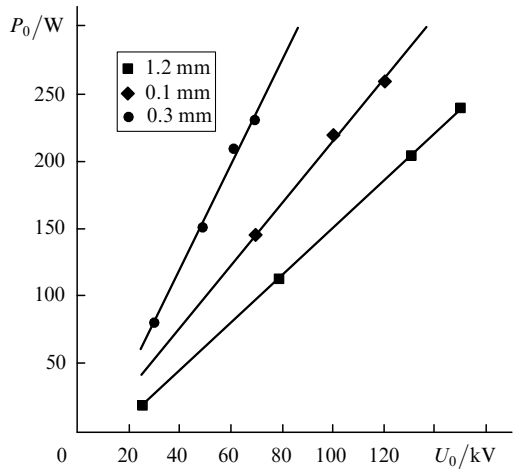

Figure 4. Dependences of the emission power P_0 of ZnSe plates of different thicknesses on the voltage U_0 for the gap between the anode and samples $z = 2$ mm.

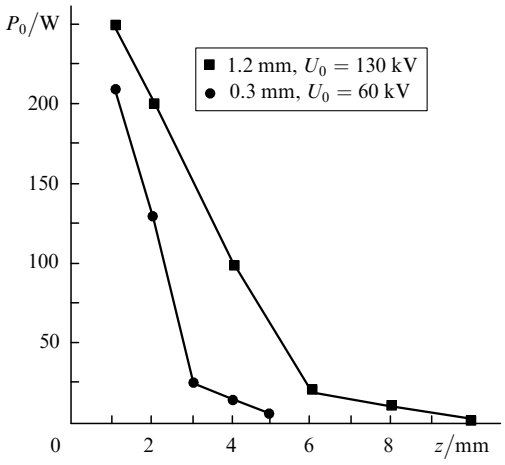

Figure 5. Dependences of the emission power P_0 of ZnSe plates of different thicknesses on the gap z for $U_0 = 130$ and 60 kV.

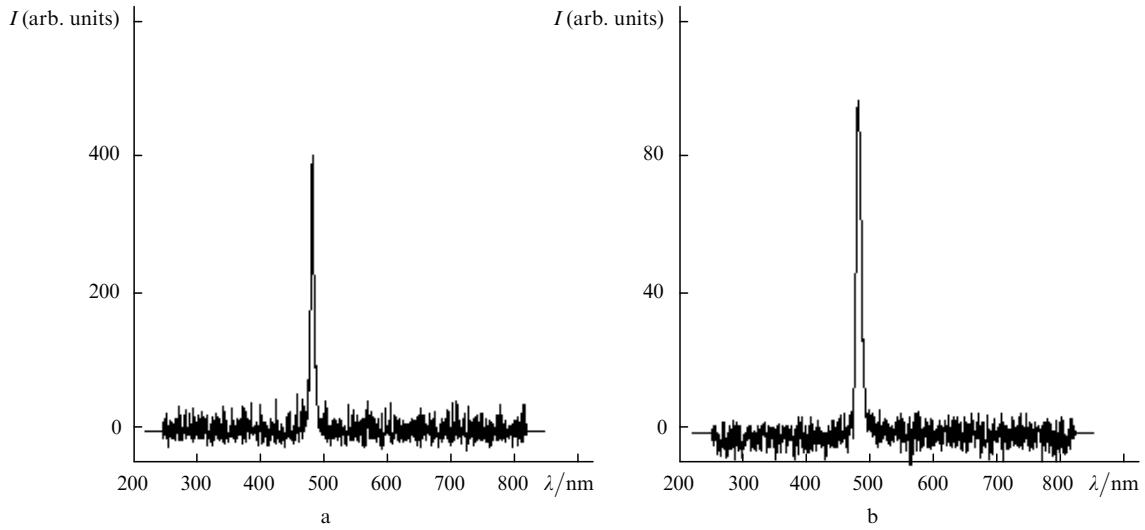

Figure 6. Lasing spectra of a 0.5-mm-thick ZnSe plate pumped by the electric field ($U_0 = 100$ kV, $z = 1.5$ mm) (a) and by the 200-keV electron beam (the beam diameter is 1 mm, the current is 5 A, and the pulse duration is 500 ps) (b).

are explained by the increase in the number of low-Q modes, the temperature shift of the emission band to the red, and a decrease in the band gap caused by the interparticle interaction in an electron–hole plasma [4, 9–11].

Figure 6 presents the lasing spectrum of a ZnSe plate pumped by an electric field and (for comparison) the emission spectrum of an electron-beam-pumped ZnSe single crystal laser. In the latter case, a chamber for electric-field pumping was replaced by a vacuum chamber with an autoemission cathode. One can see that these spectra virtually coincide. The radiation directivity improved during lasing. The divergence angle, determined from the photograph of the far-field radiation pattern, was $\sim 3^\circ$ [1].

Influence of the electrode shape. The shape of electrodes determines the direction of the lines of force of the electric field and can affect the discharge development in a semiconductor. Figure 7 shows the effect of the electrode shape on the emission of plates. The emission was always concentrated in the sites of the maximum electric field strength – usually, around the cathode boundary. As the anode diameter was increased, the discharge propagated along the plate, resembling the discharge in an amorphous dielectric (Fig. 7c). In the case of circular electrodes located above each other (Fig. 7d), lasing appeared along the perimeter of electrodes and at the centre, opposite to the conic electrode located at the centre of the circular cathode.

4. Discussion

At the electric field strength of $10^6 - 10^7$ V cm^{-1}, the concentration of electron–hole pairs caused by impact ionisation and electron tunnelling from the valence band can achieve $10^{19} - 10^{20}$ cm^{-3}. The amplification of radiation and lasing can occur in the produced dense electron–hole plasma [4, 11]. In the case of streamer lasers, such a situation appears on the front of a moving steamer with the head diameter of 1–5 μm. A discharge (streamer) propagates in this case predominantly along the crystallographic axes of the plates in the form of thin filaments of diameter 1–5 μm [3–6]. Due to the approach of the cathode and anode, the average electric filed strength in the discharge gap considerably increases, achieving 10^6 V cm^{-1}. In addition, during the discharge in air, intense microscopic flashes appear in the sites of the maximum field strength,

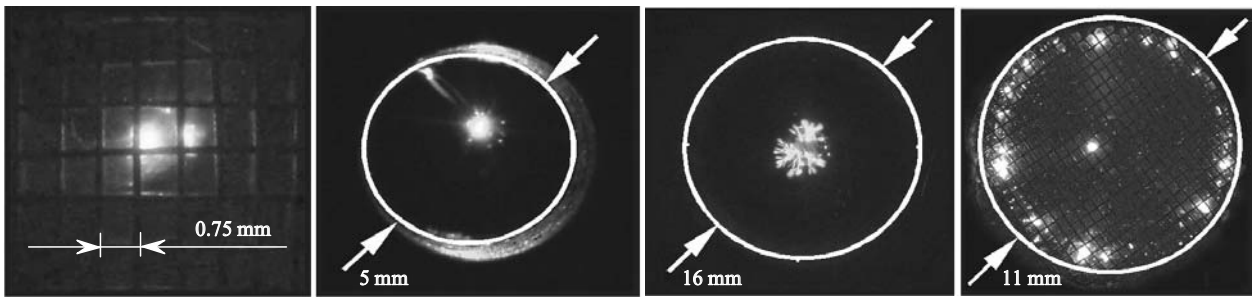

Figure 7. Emission patterns of ZnSe plates obtained with electrodes of different shapes: cathode is a truncated cone with the apex diameter $d = 1$ mm; anode is a grid with a cell step of 750 μm (a); cathode is a truncated cone with $d = 1$ mm, anode is a hollow cylinder with the internal diameter of 5 mm (b); cathode is a truncated cone with $d = 1$ mm, anode is a hollow cylinder with the internal diameter of 16 mm (c); cathode is a hollow cylinder with the internal diameter of 11 mm and the central electrode of diameter 1 mm, anode is a grid with a cell step of 750 μm (d). In all cases, $U_0 = 115$ kV and $z = 1$ mm.

for example, near the edges of the electrodes. The UV radiation of these flashes initiates a discharge in a semiconductor. As a result, the discharge propagates predominantly along the lines of force of the electric field, and the diameter of the excited region increases up to a few hundreds of micrometres, which makes it possible to increase considerable the active volume of lasers of this type. The dependences of the radiation power on the voltage pulse amplitude and the width of the gap between the sample and anode (Figs 4 and 5) are characterised by the threshold above which the lasing power drastically increases, which is typical for semiconductor lasers. In our case, the minimal threshold electric field strength was $\sim 10^3$ V cm^{-1}.

As was pointed out above, upon excitation of crystals by the electric field or electron beam (Figs 2 and 3), the light pulse shape did not correspond to the shape of the exciting voltage pulse. This can be explained by excitation of high-frequency oscillations in the coaxial attachment by the incident voltage pulse of duration 300 – 500 ps, which corresponds to the frequency $\sim$1 – 1.25 GHz, or by the kinetics of recombination emission of the electron – hole plasma. Indeed, the natural oscillation frequency of the coaxial attachment is $\sim$1.2 GHz, and therefore we can assume that the observed exponential shape of the light pulse is the envelope of a train of pulses corresponding to the decaying high-frequency oscillations of the coaxial attachment. Such a packet-pulse regime of excitation of generation in a streamer laser in a megahertz range was observed earlier in [12]. However, the possibility of the establishment of this regime is doubtful because the elongation of light pulses was also observed upon excitation of lasing by the electron beam (Fig. 3). It is most likely that the pulse elongation is caused by the kinetics of recombination emission of the electron – hole plasma. It is known that the time response of recombination emission exhibits the 'spike' structure, which is typical for free-running lasing, and can differ from the pump pulse shape [11, 13, 14]. Unfortunately, optical recording devices with a resolution of 0.5 – 1 ns used in experiments could not resolve the high-frequency 'spike' components of light pulses. To elucidate the mechanism of these phenomena, we propose to perform time-resolved measurements by using streak cameras with the nanosecond and picosecond time resolution. Experimental studies of the influence of the shape and position of electrodes on the emission pattern of semiconductors (Fig. 7) show that longitudinal (along the discharge) and transverse lasing can be achieved at many points in the crystal, which is of practical interest for the development of high-power field lasers.

Acknowledgements. The authors thank V.I. Kozlovskii and I.V. Kryukova for the discussion of results, A.F. Artemova for the preparation of samples, and A.G. Reutova for her help in experiments.

References

1. Mesyats G.A., Nasibov A.S., Shpak V.G., Shunailov S.A., Yalandin M.I. *Kvantovaya Elektron.*, **38**, 213 (2008) [*Quantum Electron.*, **38**, 213 (2008)].
2. Mesyats G.A., Korovin S.D., Sharypov K.A., et al. *Pis'ma Zh. Tekh. Fiz.*, **32**, 1 (2006).
3. Basov N.G., Molchanov A.G., Nasibov A.S., Obidin A.Z., Pechenov A.N., Popov Yu.M. *Pis'ma Zh. Eksp. Teor. Fiz.*, **19**, 650 (1974).
4. Basov N.G., Molchanov A.G., Nasibov A.S., Obidin A.Z., Pechenov A.N., Popov Yu.M. *Zh. Eksp. Teor. Fiz.*, **70**, 1751 (1976).
5. Nasibov A.S., Obidin A.Z., Pechenov A.N., Popov Yu.M. *Pis'ma Zh. Tekh. Fiz.*, **5**, 22 (1979).
6. Zubritskii V.V., Yablonskii G.P., Gribkovskii V.P. *Fiz. Tekh. Poluprovodn.*, **17**, 402 (1983).
7. Mesyats G.A., Korovin S.D., Rostov V.V., Shpak V.G., Yalandin M.I. *Proc. IEEE*, **92** (7), 1166 (2004).
8. Yalandin M.I., Shpak V.G. *Prib. Tekh. Eksp.*, (3), 5 (2001).
9. Baltrameyunas R.A., Gribkovskii V.P., Ivanov V.A., Kuokshtis E.P., Parashchyuk V.V., Yablonskii G.P. *Fiz. Tekh. Poluprovodn.*, **13**, 497 (1978).
10. Kozlovskii V.I., Nasibov A.S., Reshetov V.I. *Kvantovaya Elektron.*, **5**, 2624 (1978) [*Sov. J. Quantum Electron.*, **8**, 1477 (1978)].
11. Lysenko V.G., Revenko V.I., Tratas T.G., Timofeev V.B. *Zh. Eksp. Teor. Fiz.*, **68**, 335 (1975).
12. Gribkovskii V.P., Parashchyuk V.V., Yablonskii G.P. *Kvantovaya Elektron.*, **16**, 1145 (1989) [*Sov. J. Quantum Electron.*, **19**, 742 (1989)].
13. Nasibov A.S., Obidin A.Z., Pechenov A.N., Popov Yu.M., Frolov V.A. *Kratk. Soobshch. Fiz. FIAN*, (11), 39 (1978).
14. Obidin A.Z., Pechenov A.N., Popov Yu.M., Frolov V.A. *Kvantovaya Elektron.*, **10**, 1165 (1983) [*Sov. J. Quantum Electron.*, **13**, 746 (1983)].